

Matej Sitar · Franc Kosel · Miha Brojan

A simple method for determining large deflection states of arbitrarily curved planar elastica

Received: 8 March 2013 / Accepted: 13 September 2013 / Published online: 25 October 2013
© Springer-Verlag Berlin Heidelberg 2013

Abstract The paper discusses a relatively simple method for determining large deflection states of arbitrarily curved planar elastica, which is modeled by a finite set of initially straight flexible segments. The basic equations are built using Euler–Bernoulli and large displacement theory. The problem is solved numerically using Runge–Kutta–Fehlberg integration method and Newton method for solving systems of nonlinear equations. This solution technique is tested on several numerical examples. From a comparison of the results obtained and those found in the literature, it can be concluded that the developed method is efficient and gives accurate results. The solution scheme displayed can serve as reference tool to test results obtained via more complex algorithms.

Keywords Large deflections · Arbitrarily curved elastica · Geometrical nonlinearity · Plane deflection · Elastica problem

1 Introduction

The subject of understanding, modeling and determining large deflection behavior of flexible structures plays an important role in structural analysis and has been investigated for many years. There has always been a need to be able to compute deflections either for post-buckling analysis, estimation of rigidity of a structure or comparison of theoretical and allowable deflections, etc. For slender structural elements, which are subjected to various types of loading and can be easily deformed into states with large deflections within the range of small strains, a geometrically nonlinear analysis has to be performed to derive the equations of equilibrium [1]. Such elements can be used in engineering applications as, for example, springs, electric switch parts or partially compliant mechanisms, etc. It should be mentioned that there exist many assumptions which gave birth to theories for modeling large deflections. Namely, for slender beams, where the influence of shear stresses and the inner axial force can be neglected in comparison with the dominating inner bending moment, Euler–Bernoulli beam theory is the most appropriate and frequently used. Among the more accurate beam theories that consider the effects of shear stresses, Timoshenko and Reissner beam theories can be mentioned. For deflection of slender beams, it is known that these theories give equivalent results.

In the literature, one can find a large number of contributions pertaining to elastica problems dealing with large deflections of slender initially straight beams subjected to distributed loads or point loads acting at the

M. Sitar (✉) · F. Kosel
Laboratory for Nonlinear Mechanics, Faculty of Mechanical Engineering, University of Ljubljana,
Aškerčeva 6, 1000 Ljubljana, Slovenia
E-mail: matej.sitar@fs.uni-lj.si

M. Brojan
Department of Mechanical Engineering, Massachusetts Institute of Technology,
77 Massachusetts Avenue, Cambridge, MA 02139-4307, USA

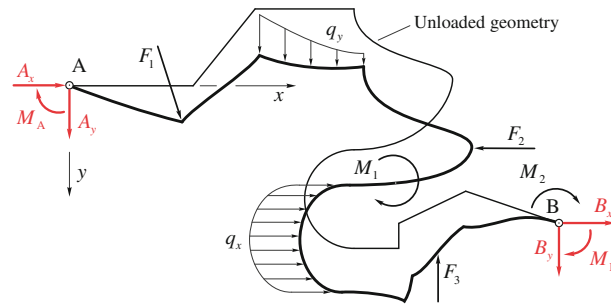


Fig. 1 Non-deflected and deflected state of curved planar elastic beam

end, e.g., [1–8]. Contrary to that, there is a much less of works studying large deflection analysis of initially curved beams, see e.g., [9–16], or publications dealing with large deflections of beam composed of several initially curved members subjected to arbitrary loading state, e.g., [17–24]. In work done by Faulkner et al. [18], the segmental shooting technique is presented. The structure is discretized into a series of segments, and the equilibrium equation is linearized within the each segment, which means each one is undergoing only small deformations. Lee et al. [19] showed post-buckling analysis of elastic frame using elliptic integral formulation. Furthermore, a homotopy method and its comparison with some other numerical methods is discussed by Watson and Wang [16]. A discrete approach is proposed by Bunce and Brown [9] and Srpčić and Saje [14], where a finite difference solutions to the governing differential equations are obtained. A useful tool for the solution of nonlinear elastica problem is also described by Somerville [13], where the quadrature matrix method is developed. Saje [23], e.g., presented a finite element formulation of an arbitrarily curved planar elastica, where formulation is based on Reissner kinematic model.

Among listed numerical procedures, some of them are simpler to understand and use than others. The same holds for their generality, efficiency and formulation. By proposing this study, we aim to present a relatively simple and efficient solution method for the determination of the large deflection states of slender, arbitrarily curved planar elastic beams. Within discretization, the beam is divided into a series of segments in which each member can be deformed into states with large deflection. These slender prismatic or non-prismatic elasticae can be in general subjected to arbitrary loading and boundary conditions. The solution method is based on a simple formulation and is therefore easy to understand and use. Furthermore, it can be generalized to employ nonlinear material response or other physical behavior without major difficulties, [1, 25–27].

2 Definition of the problem

Consider a slender arbitrarily curved elastic single branch structure of non-uniform cross section. Assume that the beam may deform only in the xy -plane. The beam, which is subjected to the various types of loads, is supported at both ends, see Fig. 1.

The material of which the beam is made is assumed to be incompressible, homogeneous, isotropic and linearly elastic. The stress–strain relationship is mathematically described by expression $\sigma(\varepsilon) = \text{sign}(\varepsilon) E |\varepsilon|$, where E is the Young’s modulus of the material.

3 Problem formulation

The elastic beam is modeled by a finite set of n initially straight flexible segments which are rigidly connected with their neighboring segments (rigidly interconnected). Each segment can be different from the other and is characterized by its constant geometry, constant loads and constant material properties.

Based on the description above, a successive beam discretization can be used;

- (i) *discretization by shape of the beam*: the beam is divided into n_m members in which their axial shapes are defined by smooth functions;
- (ii) *discretization by sections*: each member from level (i) is divided into $n_{p,k}$ sections in which their cross-sectional areas, moments of inertia (with respect to z axis), loads and material properties are defined by smooth functions, $k \in \{1, \dots, n_m\}$;

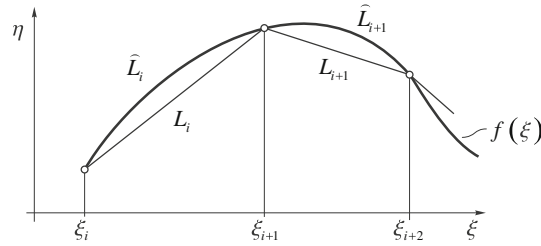


Fig. 2 Piecewise linear approximation of the nonlinear function

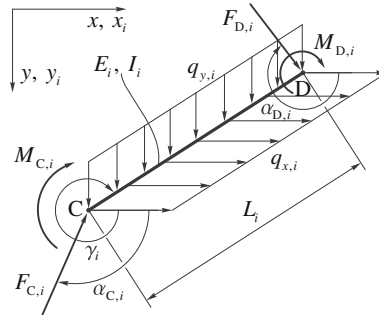


Fig. 3 *i*-th segment of the non-deflected beam

(iii) each section from level (ii) is divided into $n_{s,j}$ initially straight segments of length L_i , for which $E_i, I_i, q_i = \text{const.}, j \in \{1, 2, \dots, n_p = \sum_{k=1}^{n_m} n_{p,k}\}, i \in \{1, 2, \dots, n = \sum_{j=1}^{n_p} n_{s,j}\}$.

Note: A general smooth function from above, let's say f , defined in the local coordinate system $0\xi\eta$ is piecewise approximated by a linear function, using the relative difference between the arc length

$$\widehat{L}_i = \int_{\xi_i}^{\xi_{i+1}} \sqrt{1 + (f'(t))^2} dt \tag{1}$$

and the length of the straight line between two neighboring points, Fig. 2. The next step is to find the maximal value of integer k , such that $\xi_{i+1} = \xi_i + k\delta$, which satisfies the following inequality $(\widehat{L}_i - L_i) / \widehat{L}_i < \varepsilon_L$ within the prescribed relative error ε_L and increment δ .

Consider now a general linearly elastic segment of length L_i , which is subjected to the conservative constantly distributed loads $q_{x,i}, q_{y,i}$, moments $M_{C,i}, M_{D,i}$ and conservative point loads $F_{C,i}, F_{D,i}$ with directions defined by angles $\alpha_{C,i}, \alpha_{D,i}$, as shown in Fig. 3. Points C and D represent the starting and end points of a segment, respectively. Symbol $\gamma_i, i \in \{1, 2, \dots, n\}$, denotes the inclination of *i*-th segment of the unloaded beam.

It is obvious that $F_{D,i} = F_{C,i+1}, \alpha_{D,i} = \alpha_{C,i+1}$ and $M_{D,i} = M_{C,i+1}$ for $i \in \{1, 2, \dots, n - 1\}$.

The local Cartesian coordinate system $0x_i y_i$ is introduced such that it coincides with the global coordinate system $0xy$. The origin of the coordinate system $0xy$ is located at support A, Fig. 1. Let $s_i, 0 \leq s_i \leq L_i$, be the curvilinear coordinate along the longitudinal axis of the elastic segment measured from the starting point C and $\vartheta_i(s_i)$ be the angle of inclination between the positive part of the x axis and tangent to the neutral axis of *i*-th segment at the local point s_i .

Static equilibrium of an infinitesimal element of the deflected segment, cf. [1], together with geometrical relations

$$dx_i/ds_i = x'(s_i) = \cos \vartheta_i(s_i) \quad \text{and} \quad dy_i/ds_i = y'(s_i) = \sin \vartheta_i(s_i) \tag{2}$$

and expression $M_i(s_i) = E_i I_i \vartheta_i'(s_i)$, where I_i represents an area moment of inertia of *i*-th segment, results in

$$E_i I_i \vartheta_i''(s_i) + F_{x,i}(s_i) \sin \vartheta_i(s_i) + F_{y,i}(s_i) \cos \vartheta_i(s_i) = 0. \tag{3}$$

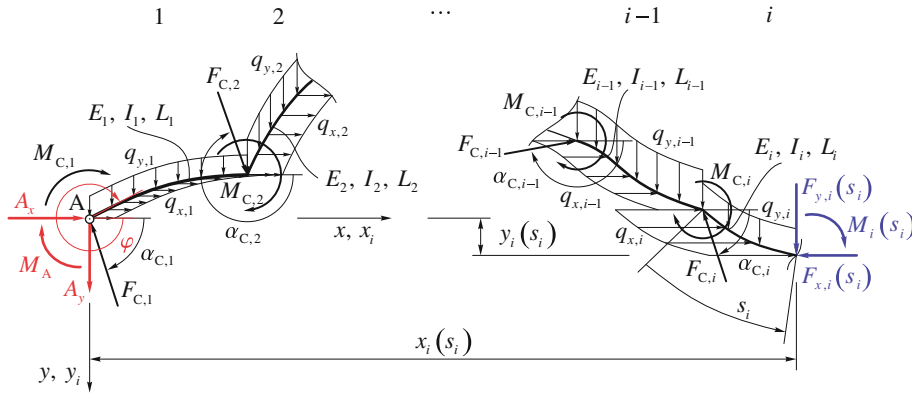


Fig. 4 Cut off part of the deflected beam

The governing differential equation (3) together with the accompanying boundary conditions characterizes the large deflection behavior of i -th segment subjected to the constantly distributed loads, moments and conservative point loads at both ends. The inner forces $F_{x,i}(s_i)$ and $F_{y,i}(s_i)$ are determined from the static equilibrium in the cut off part of the deflected beam over i -th segment at s_i , see Fig. 4.

Accordingly

$$F_{x,i}(s_i) = +A_x - F_{C,i} \cos \alpha_{C,i} + q_{x,i}s_i + \sum_{k=1}^{i-1} (-F_{C,k} \cos \alpha_{C,k} + q_{x,k}L_k) \quad (4)$$

and

$$F_{y,i}(s_i) = -A_y + F_{C,i} \sin \alpha_{C,i} - q_{y,i}s_i + \sum_{k=1}^{i-1} (F_{C,k} \sin \alpha_{C,k} - q_{y,k}L_k) \quad (5)$$

for $i \in \{1, 2, \dots, n\}$.

The set of governing second order nonlinear differential equations (3), for $i \in \{1, 2, \dots, n\}$, is solved numerically using Runge–Kutta–Fehlberg (RKF) integration method, cf. [28], together with accompanying initial conditions

$$\vartheta_i(s_i = 0) = \begin{cases} \varphi & \text{for } i = 1, \\ \Delta\gamma_{i-1} + \vartheta_{i-1}(L_{i-1}) & \text{for } i \in \{2, 3, \dots, n\}. \end{cases} \quad (6)$$

and

$$\vartheta'_i(s_i = 0) = \begin{cases} \mu & \text{for } i = 1, \\ -\frac{M_{C,i}}{E_i I_i} + \frac{E_{i-1} I_{i-1}}{E_i I_i} \vartheta'_{i-1}(L_{i-1}) & \text{for } i \in \{2, 3, \dots, n\}. \end{cases} \quad (7)$$

where $\Delta\gamma_i = \gamma_{i+1} - \gamma_i, i \in \{1, 2, \dots, n - 1\}$, represent the change of the angle of inclination between two neighboring segments. φ is the unknown angle of inclination of the deformed beam at $s_1 = 0$ and $\mu = -M_{C,1}/(E_1 I_1)$ in the case of hinged support A. In the second case, where support A is clamped, $\varphi = \gamma_1$ and μ is the unknown curvature of the deformed beam, Fig. 4. Since there are up to three unknown parameters in the numerical calculation, i.e., A_x, A_y and φ or μ , the solutions of $\vartheta_i(s_i)$ are obtained by employing Newton method for a system of nonlinear equations, cf. [28]. Additional conditions relate to support B and are in general written as

$$\begin{aligned} \vartheta'_n(s_n = L_n) &= M_{D,n}/(E_n I_n), \\ \vartheta_n(s_n = L_n) &= \gamma_n, \\ x_n(s_n = L_n) &= \sum_{i=1}^n L_i \cos \gamma_i, \\ y_n(s_n = L_n) &= \sum_{i=1}^n L_i \sin \gamma_i, \end{aligned} \quad (8)$$

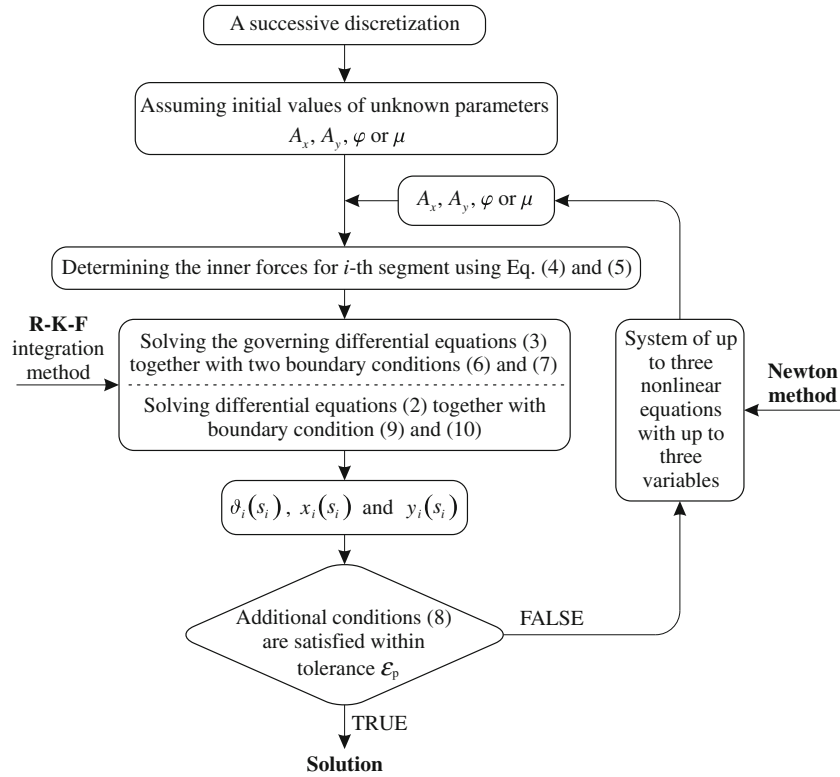


Fig. 5 Flowchart of the numerical procedure

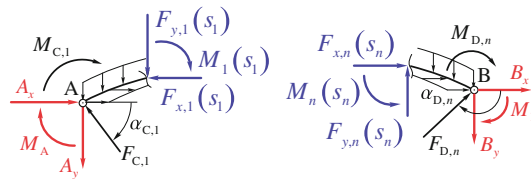


Fig. 6 Determining the reaction forces and moments

if the support is hinged, or clamped, and if the support constrains displacements in the horizontal direction or in the vertical direction, respectively. It should be mentioned that the Jacobian matrix in Newton method is generated using numerical differentiations at fixed increments $\Delta A_x, \Delta A_y, \Delta \varphi$ or $\Delta \mu$ ($= 10^{-8}$). The deflected states of the segments can be determined from geometrical relations (2) together with boundary conditions

$$x_i(s_i = 0) = \begin{cases} 0 & \text{for } i = 1, \\ x_{i-1}(L_{i-1}) & \text{for } i \in \{2, 3, \dots, n\}. \end{cases} \quad (9)$$

and

$$y_i(s_i = 0) = \begin{cases} 0 & \text{for } i = 1, \\ y_{i-1}(L_{i-1}) & \text{for } i \in \{2, 3, \dots, n\}. \end{cases} \quad (10)$$

A more detailed numerical procedure is presented graphically in Fig. 5.

When the solution of the problem is obtained, the remaining reaction forces and moments can be determined by the following expressions, cf. Fig. 6,

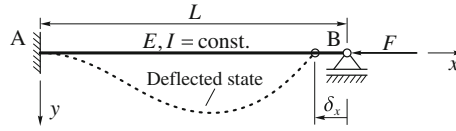


Fig. 7 III Euler column

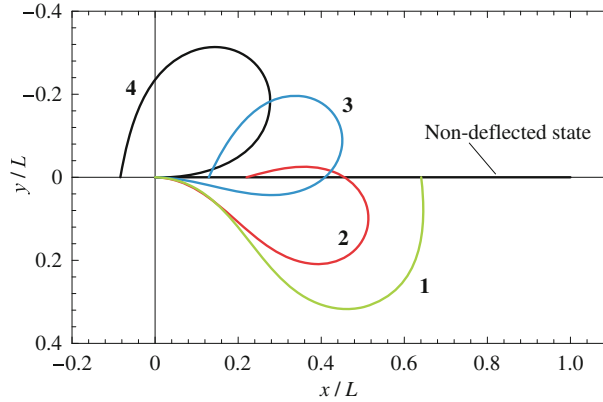


Fig. 8 Deflected states of III Euler column ($n = 1$)

Table 1 Displacement δ_x at support B for III Euler column compared with that in [6]

i	λ	δ_x/L	δ_x/L [6]
1	22.751	0.35933	0.360
2	6.923	0.77996	0.780
3	-12.055	0.87072	0.871
4	-11.312	1.08367	1.084

$$M_A = -E_1 I_1 \vartheta_1'(s_1 = 0) - M_{C, 1}, \tag{11}$$

$$B_x = -F_{x, n}(s_n = L_n) + F_{D, n} \cos \alpha_{D, n}, \tag{12}$$

$$B_y = F_{y, n}(s_n = L_n) + F_{D, n} \sin \alpha_{D, n}, \tag{13}$$

$$M_B = E_n I_n \vartheta_n'(s_n = L_n) - M_{D, n}. \tag{14}$$

4 Numerical examples

Based on the numerical procedure presented above, the deflected states for various problems are shown in this section. Additional conditions are satisfied within a tolerance $\epsilon_p = 10^{-8}$.

4.1 III Euler case

Consider a hinged–clamped prismatic beam subjected to axial force F , see Fig. 7, which is defined by expression $F = \lambda EI/L^2$. Constant λ represents load factor. The same problem, which is also known as III Euler column, was investigated by Levyakov and Kuznetsov [6], where the exact elastica solutions expressed in terms of Jacobi elliptic functions were used. The deflected states are shown in Fig. 8 and the results of the determined displacement δ_x obtained by our method and the method presented in [6] are listed in Table 1. A good agreement of results is observed.

4.2 Square frame

Mattiasson [21] presented highly accurate results for some large deflection problems analyzed by means of elliptic integrals. One of them is a square frame loaded at the midpoints of a pair of opposite sides, see Fig. 9a.

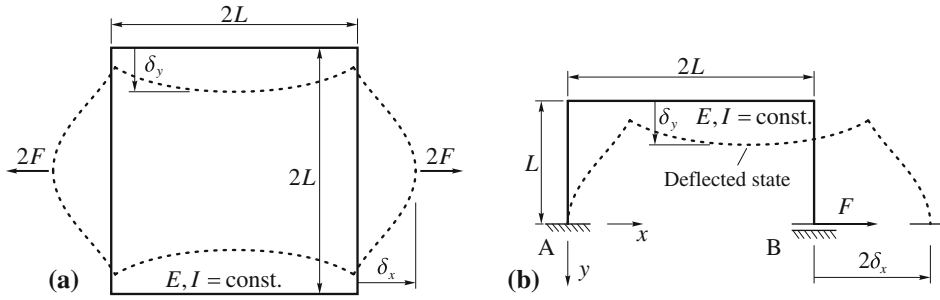


Fig. 9 Square frame

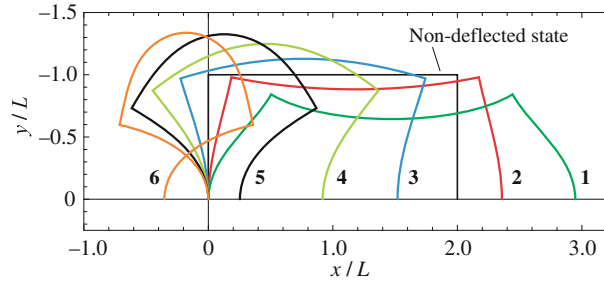


Fig. 10 Deflected states of square frame ($n = 3$)

Table 2 Displacement δ_x and δ_y for a square frame compared with that in Ref. [21]

i	λ	δ_x/L	δ_x/L [21]	δ_y/L	δ_y/L [21]
1	4.0	0.47375	0.47375	0.35581	0.35581
2	1.0	0.17889	0.17889	0.11699	0.11699
3	-1.0	-0.24025	-0.24025	0.12850	0.12850
4	-2.0	-0.54087	-0.54087	-0.24854	-0.24854
5	-3.0	-0.87339	-0.87339	-0.32561	-0.32561
6	-4.0	-1.17703	-1.17703	-0.33754	-0.33754

Since it is a symmetrical problem, both ends of a half of the frame can be clamped, where in order to satisfy the conditions of symmetry, displacement of one support in the x direction is left free, Fig. 9b. As in the previous example, the frame is loaded by load $F = \lambda EI/L^2$. Deflected states are shown in Fig. 10 whereas the results of the determined displacement δ_x and δ_y obtained by our method and results given in [21] are listed in Table 2.

It is found that the results of both methods are in excellent agreement.

4.3 Half circular arch

Consider a half circular arch of radius R and uniform cross section. The beam is subjected to a constantly distributed load $q_y = \lambda EI/R^3$, see Fig. 11. The deflected states depending upon the number of segments n , where $L_i = \text{const.}$ for $i \in \{1, 2, \dots, n\}$, are shown in Fig. 12 and Table 3.

In order to validate the presented method, the governing differential equation describing the large deflection behavior of a simply supported uniform curvature beam subjected to constantly distributed load q_y , i.e.,

$$EI\vartheta''(s) + q_y \left(\frac{\pi R}{2} - s \right) \cos \vartheta(s) = 0, \tag{15}$$

together with boundary conditions $\vartheta'(s=0) = 1/R$ and $\vartheta'(s=\pi R) = 1/R$ was solved using RKF and one parameter shooting method (OPS). The expression for the inner moment is given as $M(s) = EI(\vartheta'(s) - 1/R)$, [10].

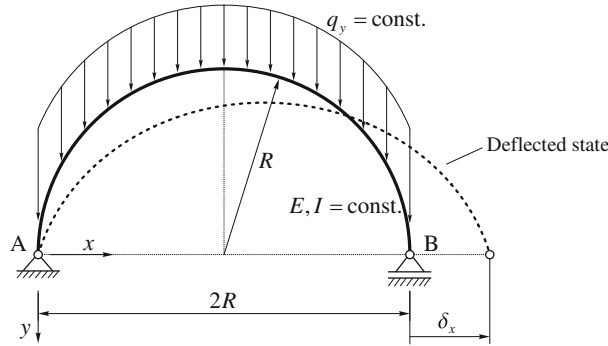


Fig. 11 Half circular arch

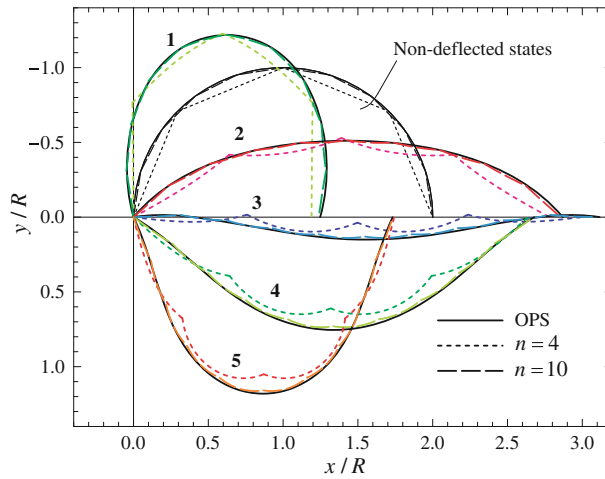


Fig. 12 Deflected states of a half circular arch (one parameter shooting method, $n = 4$ and $n = 10$)

Table 3 Displacement δ_x at support B for a half circular arch compared with that obtained by one parameter shooting method (OPS)

i	λ	$\delta_{x,n=4}/R$	$\delta_{x,n=10}/R$	$\delta_{x,n=90}/R$	$\delta_{x,n=360}/R$	$\delta_{x,OPS}/R$
1	-4.0	-0.80986	-0.76162	-0.75252	-0.75242	-0.75241
2	0.65	0.77953	0.85491	0.86960	0.86977	0.86978
3	1.10	0.99463	1.09660	1.11595	1.11618	1.11620
4	2.00	0.63538	0.67245	0.67881	0.67889	0.67889
5	5.50	-0.25779	-0.26595	-0.26741	-0.26743	-0.26743

4.4 Tapered and prismatic angle frame

An angle frame subjected to a point load $F = \lambda EI/L^2$ is composed of prismatic and non-prismatic members as shown in Fig. 13. The non-prismatic member has a tapered longitudinal shape, where $I(\eta)$ is defined as

$$I(\eta) = I(\eta = 0) \left(1 + \frac{3}{L}\eta\right)^3 \tag{16}$$

and is divided into $n_{s,3}$ segments of equal length, which is determined by discretization of Eq. (16), see Fig. 13, i.e.,

$$I_i = I \left(1 + \frac{3}{n_{s,3}} \left(i - \frac{1}{2}\right)\right)^3, \quad i \in \{1, 2, \dots, n_{s,3}\} \tag{17}$$

Deflected states upon the number of segments $n_{s,3}$ are shown in Fig. 14, Tables 4 and 5.

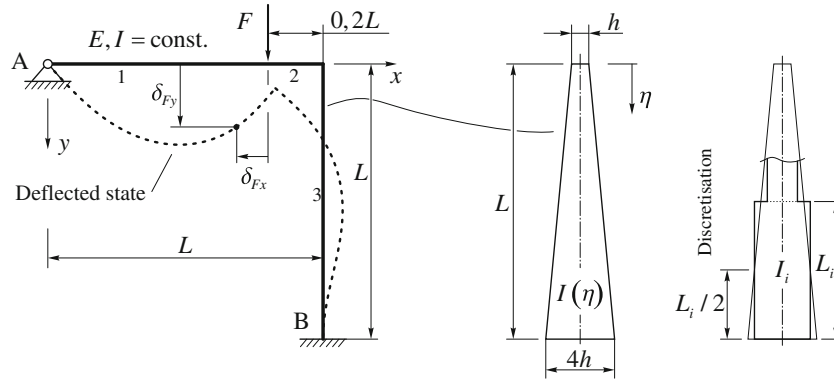


Fig. 13 Tapered angle frame

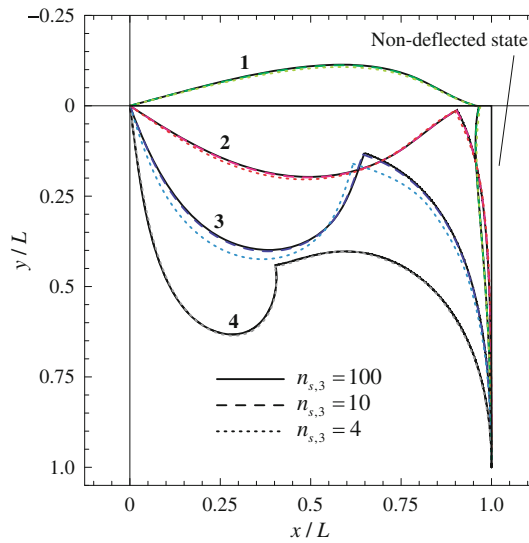


Fig. 14 Deflected states of tapered angle frame ($n = 6, n = 12$ and $n = 102$)

Table 4 Displacement δ_{F_x} for a tapered angle frame obtained by presented method

i	λ	$\delta_{F_x, n_{s,3}=4}/L$	$\delta_{F_x, n_{s,3}=10}/L$	$\delta_{F_x, n_{s,3}=100}/L$
1	-50.0	0.01512	0.01631	0.01671
2	30.0	0.06434	0.05974	0.05862
3	60.0	0.26079	0.23705	0.23334
4	125.0	0.46244	0.46235	0.46280

Table 5 Displacement δ_{F_y} for a tapered angle frame obtained by presented method

i	λ	$\delta_{F_y, n_{s,3}=4}/L$	$\delta_{F_y, n_{s,3}=10}/L$	$\delta_{F_y, n_{s,3}=100}/L$
1	-50.0	-0.07448	-0.07878	-0.08017
2	30.0	0.12965	0.12825	0.12761
3	60.0	0.34323	0.31628	0.31190
4	125.0	0.62294	0.61838	0.61818

If now support B is considered as a hinged support and the non-prismatic member as prismatic, where $I(\eta) = I$, the Lee frame can be obtained, cf. [19]. The graph of equilibrium solution's function which is represented by the relation between the load parameter λ and vertical or horizontal displacement δ_{F_x} or δ_{F_y} , respectively, Fig. 13, is for the Lee frame presented in Fig. 15 and listed in Table 6.

A good agreement of results between our method and the method presented in [19] is observed.

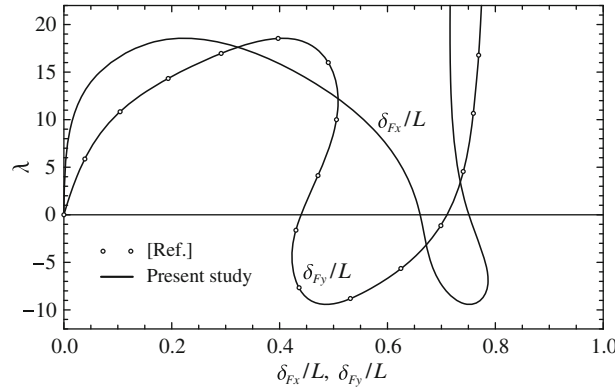


Fig. 15 λ - δ_{F_x}/L and λ - δ_{F_y}/L curves ($n = 3$)

Table 6 Displacement δ_{F_x} and δ_{F_y} for the Lee frame

i	λ	δ_{F_x}/L	δ_{F_y}/L
1	12.0	0.02892	0.12872
2	18.55874	0.22398	0.40610
3	12.0	0.51343	0.50843
4	0.0	0.66061	0.43972
5	-9.42129	0.75175	0.48498
6	0.0	0.75099	0.71072
7	12.0	0.71831	0.76198
8	20.0	0.71596	0.77247

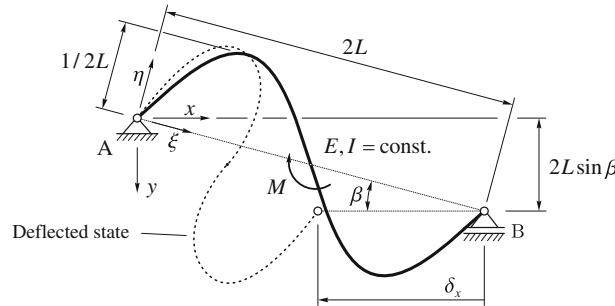


Fig. 16 Inclined sinusoidal beam

4.5 Inclined sinusoidal beam

A sinusoidal beam, which is described by function $f(\xi) = \frac{L}{2} \sin\left(\frac{\pi}{2L}\xi\right)$, $0 \leq \xi \leq 2L$, is inclined to the positive part of the x axis at an angle $\beta = 15^\circ$ and is subjected to the moment $M = \lambda EI/L$ at midpoint, $\xi = L$, as shown in Fig. 16. The beam is discretized by $n = 84$ initially straight segments, where a relative error $\varepsilon_L = 10^{-4}$ and increment $\delta = 5 \times 10^{-5}L$ were used. The deflected states are shown in Fig. 17, and the results of the determined displacement δ_x obtained by our method are listed in Table 7.

4.6 Composed beam

A composed beam assembled from polygon lines, a circular arch and sinusoidal curve, which is described by the function $f(\xi) = L \sin\left(\frac{\pi}{2L}\xi\right)$, $0 \leq \xi \leq 2L$, is subjected to a constantly distributed load $q_y = \lambda EI/L^3$ and conservative force $F = 0.2q_y L$, see Fig. 18. The deflected states are shown in Fig. 19, and the results of the determined displacements δ_x and δ_y obtained by our method are listed in Table 8. Here, the circular arch is discretized by $n_{s,2} = 34$ initially straight segments of equal length, whereas the sinusoidal member is discretized by $n_{s,4} = n_{s,5} = 21$ segments ($\varepsilon_L = 10^{-4}$, $\delta = 5 \times 10^{-5}L$).

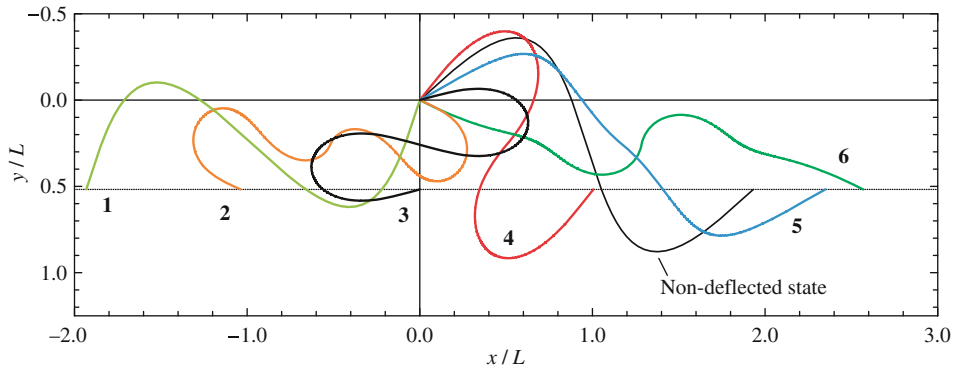


Fig. 17 Deflected states of inclined sinusoidal beam ($n = 84$)

Table 7 Displacement δ_x for the inclined sinusoidal beam

i	λ	δ_x/L
1	0.0	3.86370
2	-15.0	2.96983
3	0.0	1.93185
4	1.865	0.92634
5	-2.0	-0.41717
6	-10.0	-0.63640

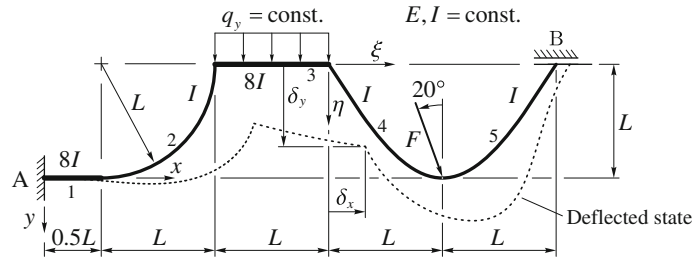


Fig. 18 Composed beam

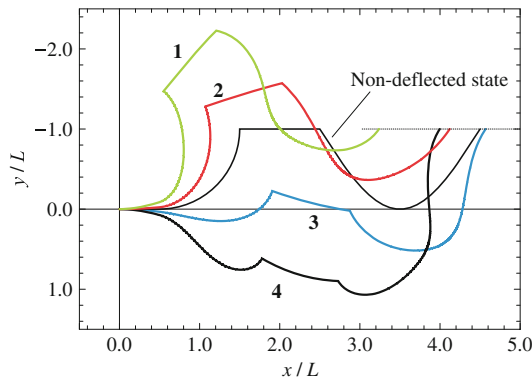


Fig. 19 Deflected states of composed beam ($n = 78$)

As it can be noticed, the results obtained in this study are in good agreement with those found in literature.

5 Conclusion

A relatively simple and efficient numerical method for determining large deflection states of arbitrarily curved planar elastic beams, which are subjected to arbitrary loading and boundary conditions, is presented in this

Table 8 Displacement δ_x and δ_y for the composed beam

i	λ	δ_x/L	δ_y/L
1	8.8	-1.29219	-1.22785
2	-2.0	-0.47120	-0.57211
3	3.0	0.37516	1.02024
4	8.8	0.22912	1.89770

paper. The advantages of proposed method are its simplicity and generality of formulation. The beam is divided into a series of segments, where each of them can be deformed into large deflections states. This means the beam may be discretized into less segments, especially for initially straight parts of the beam, where only one segment may be sufficient. The boundary-value problem is transformed to a series of initial-value problems. In comparison with a classical finite element method or any other, which is more complex, the proposed method is easy to understand and can be employed without any additional difficulties even if the material exhibits nonlinear response or any other physical behavior. A disadvantage of the proposed method may be the need of solving nonlinear differential equation for each segment of the beam in each iteration step of the Newton method—but should not be too cumbersome for modern desktop computers. Furthermore, the selection of initial conditions may be in some cases problematic. Nevertheless, this can be easily avoided by employing the loads changing incrementally.

An aspect of finding special points and branches of solution on a characteristic curve (an important task, especially in stability analysis) was not covered in this study. A continuation algorithm could, e.g., be incorporated and thus supplement the proposed method to make it even more universal. Our primary attempt was to set up a simple, quick to learn, and efficient method for finding large deflection states of beams, which can be used alone, and/or as an auxiliary tool to check results obtained via more complex or any other novel algorithms.

Conflict of interest The authors declare that they have no conflict of interest.

References

- Brojan, M., Sitar, M., Kosel, F.: On static stability of nonlinearly elastic Euler's columns obeying the modified Ludwick's Law. *Int. J. Struct. Stab. Dyn.* **12**(6), 1250077 (1)–1250077 (19) (2012)
- Campanile, L.F., Hasse, A.: A simple and effective solution of the elastica problem. *J. Mech. Eng. Sci.* **222**(12), 2513–2516 (2008)
- Chen, L.: An integral approach for large deflection cantilever beams. *Int. J. Non-Linear Mech.* **45**, 301–305 (2010)
- Dado, M., Al-Sadder, S.: A new technique for large deflection analysis of non-prismatic cantilever beams. *Mech. Res. Commun.* **32**(6), 692–703 (2005)
- Holden, J.T.: On the finite deflections of thin beams. *Int. J. Solid Struct.* **8**(8), 1051–1055 (1972)
- Levyakov, S.V., Kuznetsov, V.V.: Stability analysis of planar equilibrium configurations of elastic rods subjected to end loads. *Acta Mech.* **211**(1–2), 73–87 (2010)
- Vaz, M.A., Silva, D.F.C.: Post-buckling analysis of slender elastic rods subjected to terminal forces. *Int. J. Non-Linear Mech.* **38**(4), 483–492 (2003)
- Wang, C.Y.: Post-buckling of a clamped-simply supported elastica. *Int. J. Non-Linear Mech.* **32**(6), 1115–1122 (1997)
- Bunce, J.W., Brown, E.H.: Non-linear bending of thin, ideally elastic rods. *Int. J. Mech. Sci.* **18**(9–10), 435–441 (1976)
- De Bona, F., Zelenika, S.: A generalized elastica-type approach to the analysis of large displacements of spring-strips. *J. Mech. Eng. Sci.* **211**(7), 509–517 (1997)
- Nallathambi, A.K., Rao, C.L., Srinivasan, S.M.: Large deflection of constant curvature cantilever beam under follower load. *Int. J. Mech. Sci.* **52**, 440–445 (2010)
- Shinohara, A.: Large deflection of a circular C-shaped spring. *Int. J. Mech. Sci.* **21**, 179–186 (1979)
- Somerville, I.: Quadrature matrices and elastica problems. *Comp. Method App. Mech. Eng.* **69**(3), 345–354 (1988)
- Srpčič, S., Saje, M.: Large deformations of thin curved plane beam of constant initial curvature. *Int. J. Mech. Sci.* **28**(5), 275–287 (1986)
- Wang, C.Y., Watson, L.T.: On the large deformations of C-shaped springs. *Int. J. Mech. Sci.* **22**, 395–400 (1980)
- Watson, L.T., Wang, C.Y.: A homotopy method applied to elastica problems. *Int. J. Solids Struct.* **17**(1), 29–37 (1981)
- Dado, M., Al-Sadder, S.: The elastic spring behavior of a rhombus frame constructed from non-prismatic beams under large deflection. *Int. J. Mech. Sci.* **48**, 958–968 (2006)
- Faulkner, M.G., Lipsett, A.W., Tam, V.: On the use of a segmental shooting technique for multiple solutions of planar elastica problems. *Comp. Methods App. Mech. Eng.* **110**(3–4), 221–236 (1993)
- Lee, S.L., Manuel, F.S., Rossow, E.C.: Large deflections and stability of elastic frames. *J. Eng. Mech. Div.* **94**(2), 521–548 (1968)

20. Manuel, F.S., Lee, S.L.: Flexible bars subjected to arbitrary discrete loads and boundary conditions. *J. Franklin Inst.* **285**(6), 452–474 (1968)
21. Mattiasson, K.: Numerical results from large deflection beam and frame problems analysed by means of elliptic integrals. *Int. J. Num. Methods Eng.* **17**(1), 145–153 (1981)
22. Phungpaingam, B., Chucheeepsakul, S.: Postbuckling of elastic beam subjected to a concentrated moment within span length of beam. *Acta Mech.* **23**(3), 287–296 (2007)
23. Saje, M.: Finite element formulation of finite planar deformation of curved elastic beams. *Comput. Struct.* **39**(3–4), 327–337 (1991)
24. Thacker, W.I., Wang, C.Y., Watson, L.T.: Effect of flexible joints on the stability and large deflections of a triangular frame. *Acta Mech.* **200**(1–2), 11–24 (2008)
25. Brojan, M., Cebren, M., Kosel, F.: Large deflections of non-prismatic nonlinearly elastic cantilever beams subjected to non-uniform continuous load and a concentrated load at the free end. *Acta Mech. Sin.* **28**(3), 863–869 (2012)
26. Brojan, M., Kosel, F.: Approximative formula for post-buckling analysis of nonlinearly elastic columns with superellipsoidal cross-sections. *J. Reinf. Plast. Comp.* **30**(5), 409–415 (2011)
27. Brojan, M., Videnic, T., Kosel, F.: Large deflections of nonlinearly elastic non-prismatic cantilever beams made from materials obeying the generalized Ludwick constitutive law. *Meccanica* **44**, 733–739 (2009)
28. Burden, R.L., Faires, J.D.: *Numerical Analysis*, 9th ed. Brooks/Cole, Boston (2010)